Developments in resistivity inversion with electrode displacements for landslide monitoring

M.H.Loke (Geotomo Software Sdn Bhd)

P. B. Wilkinson, J.E. Chambers, S. Uhlemann and P.I. Meldrum

(British Geological Survey)

Email : drmhloke@yahoo.com

Outline

1. Geoelectrical surveys for landslide monitoring
2. Least-squares inversion and Jacobian matrix calculation methods
3. 2-D synthetic example
4. 2-D and 3-D field examples
5. Conclusions

Geoelectrical surveys for landslide monitoring

1. Repeated measurements are used to detect temporal changes in the subsurface below unstable slopes.

2. Positions of the electrodes are measured at the start, but electrode positions as well as subsurface resistivity change with time. Both resistivity and electrode positions have to be estimated from apparent resistivity data alone.

3. Direction of movement is unidirectional – downslope. Amount of movement variable, depending on slope and geology.

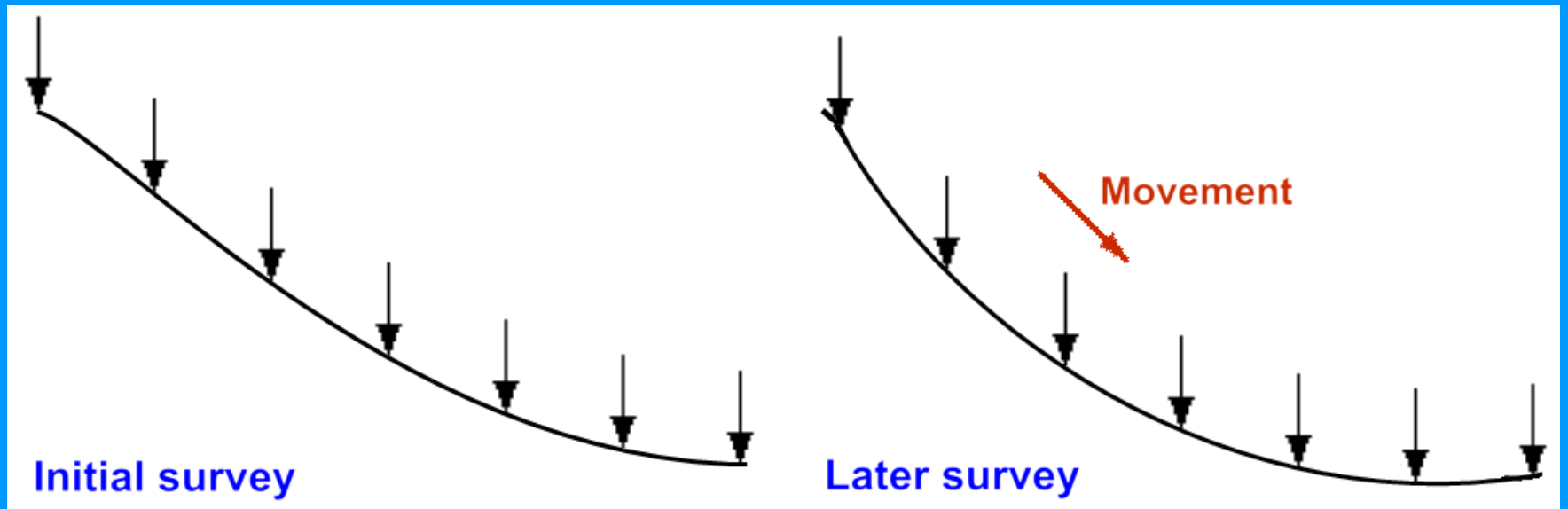

Information available and parameters needed

Information available:-

1). Apparent resistivity data and exact electrode positions from initial survey.

2). Apparent resistivity data from later time survey.

3). Electrodes will only move downslope.

Parameters to calculate:-

1). Subsurface resistivity for both surveys.

2). Electrode positions for later survey. Changes must be consistent with slope direction.

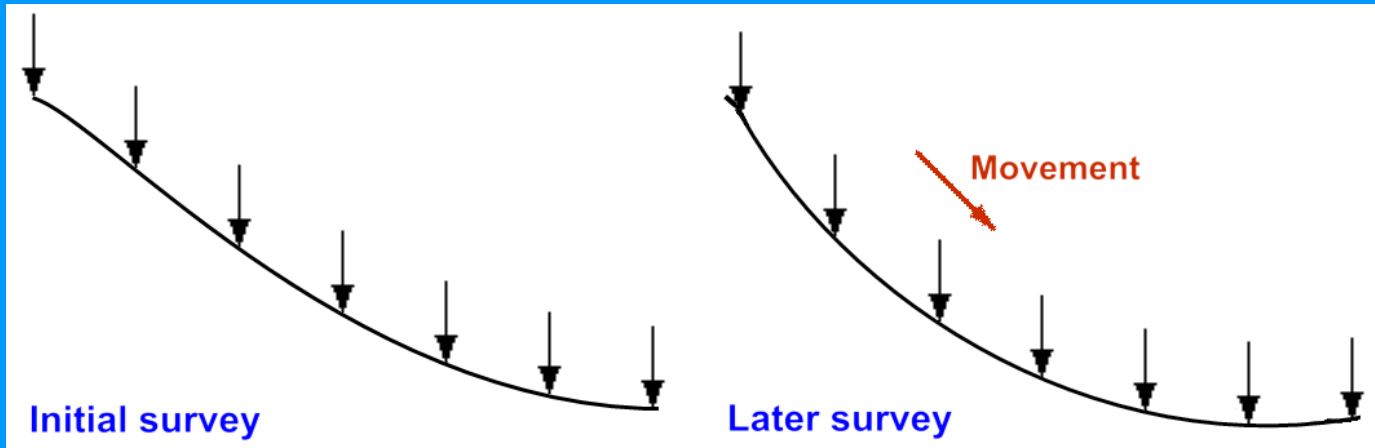

The least-squares optimization method

The smoothness-constrained least-squares method is commonly used in 2-D and 3-D resistivity inversion, using the following equation.

$$\left[\mathbf{J}_i^T\mathbf{R}_d\mathbf{J}_i + \lambda_i\mathbf{W}^T\mathbf{R}_m\mathbf{W}\right]\Delta\mathbf{r}_i = \mathbf{J}_i^T\mathbf{R}_d\mathbf{g}_i - \lambda_i\mathbf{W}^T\mathbf{R}_m\mathbf{W}\mathbf{r}_{i-1}$$

$\mathbf{W}$ = roughness filter, λ = roughness filter damping factor

$\mathbf{r}_{i-1}$ = current inversion model, $\Delta\mathbf{r}_i$ = change in model resistivity

$\mathbf{R}_m$, $\mathbf{R}_d$ = model and data weighting matrices

$\mathbf{g}$ = data misfit, $\mathbf{J}$ = Jacobian matrix of partial derivatives.

Model parameter vector $\mathbf{r}$ normally contains the (logarithm) of the model resistivity values. It can be modified to include the electrode positions.

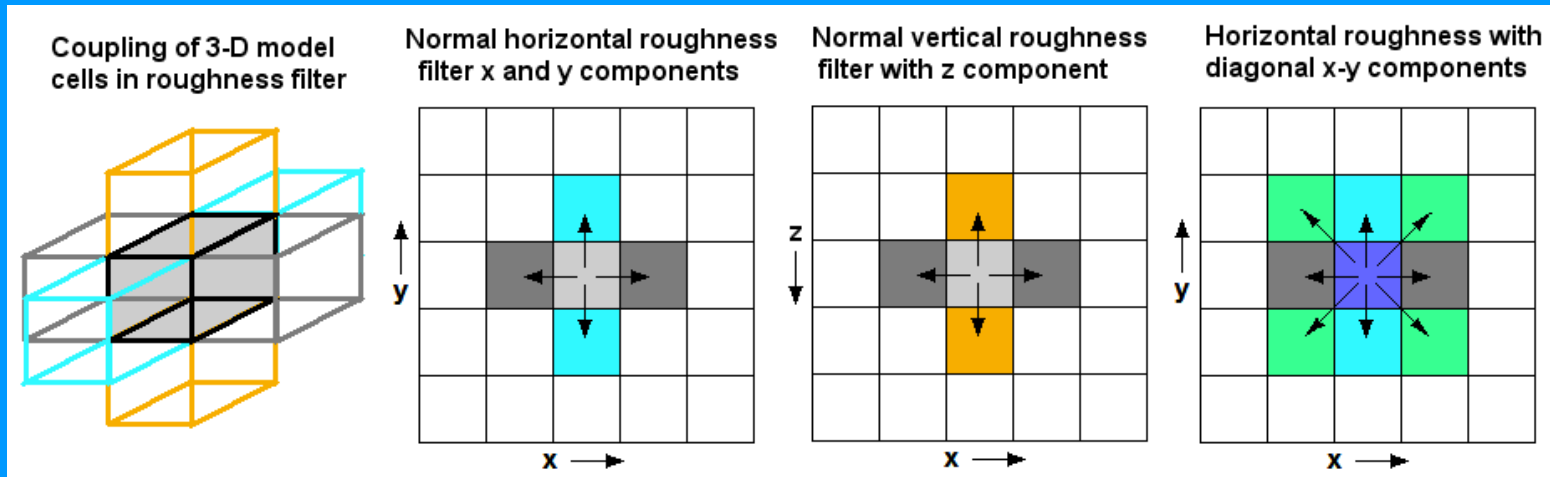

Modified least-squares optimization method

The modified least-squares to incorporate the (x,z) positions.

$$\left[\mathbf{G}_{i-1}^{T}\mathbf{R}_{d}\mathbf{G}_{i-1}+\lambda_{i}^{2}\left(\mathbf{V}^{T}\mathbf{R}_{m}\mathbf{V}+\delta\mathbf{I}\right)\right]\Delta\mathbf{q}_{i}=\mathbf{G}_{i-1}^{T}\mathbf{R}_{d}\mathbf{g}_{i-1}-\lambda_{i}^{2}\left(\mathbf{V}^{T}\mathbf{R}_{m}\mathbf{V}+\delta\mathbf{I}\right)\left(\mathbf{q}_{i-1}-\mathbf{q}_{0}\right)$$

New model parameters vector $\mathbf{q}=\begin{pmatrix}\mathbf{r}\\ \mathbf{x}\\ \mathbf{z}\end{pmatrix}$ **, Jacobian matrix G = (J X Z)**

X and Z are the partial derivatives of the apparent resistivity values with respect to changes in the (x,y) electrode positions.

New roughness filter term V = (W αW_x βW_y). W_x and W_y are the roughness filters for x and z with damping factors α and β . A reference model damping term δ is also added.

There are 2 issues that needs to be resolved :-

1). Calculation of the spatial Jacobian matrices X and Z.

2). Finding optimum values for the damping factors α and β .

Calculating the spatial Jacobian matrices

X matrix contains the change in the potential Φ due to a change the *x* position of the electrode, such as $\partial \Phi_i / \partial x_k$.

Sensitivity values are calculated with the 'adjoint-equation' method. The potentials values are calculated using the finite-element method by solving the matrix equation : - CΦ = s .

C = capacitance matrix that contains mesh resistivity and shapes

Φ = nodes potential vector, s = nodes current vector

For a single mesh element $c_{pq} = k_{pq}(x,z)\sigma_j$, σ_j is cell conductivity. The $k_{pq}(x,z)$ term depends on the coordinates at the corners of the cell.

(a)

(b)

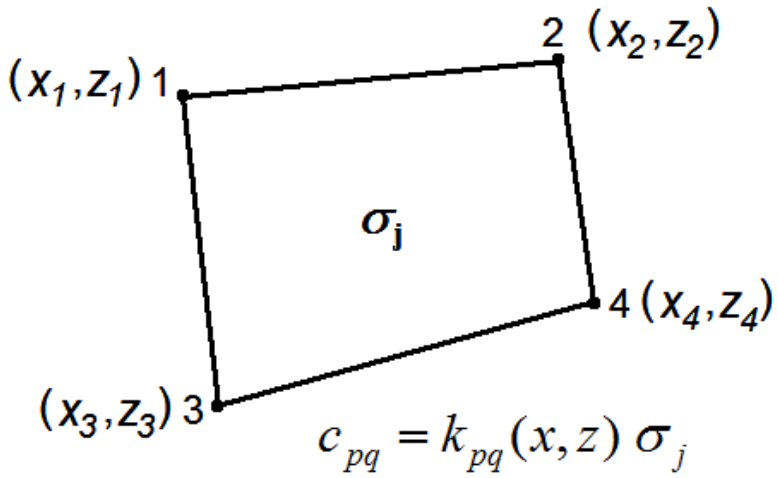

Adjoint-equation method

Differentiation of the capacitance matrix equation $\mathbf{C\Phi = s}$ wrt the x-position of an electrode gives

$$\mathbf{C}\frac{\partial \mathbf{\Phi}}{\partial x_k} = -\frac{\partial \mathbf{C}}{\partial x_k}\mathbf{\Phi}$$

All the information needed to calculate $\partial\mathbf{\Phi}/\partial x_k$ is available after calculating the potentials $\mathbf{\Phi}$. $\partial\mathbf{C}/\partial x_k$ can be calculated from $c_{pq} = k_{pq}(x,z)\sigma_j$ such as,

$$\frac{\partial c_{pq}}{\partial x_k} \approx \frac{k_{pq}(x_k + \Delta x_k, z) - k_{pq}(x_k - \Delta x_k, z)}{2\Delta x_k}\sigma_j$$

Each row in the $\mathbf{C}$ matrix has 9 (or less) non-zero elements for a 2-D mesh. Only a small number of rows in $\partial\mathbf{C}/\partial x_k$ matrix are affected by a shift in an electrode. The non-zero rows are multiplied by the $\mathbf{\Phi}$ vector to obtain $\partial\mathbf{\Phi}/\partial x_k$.

Computer time is greatly reduced by only calculating the $\mathbf{C}$ matrix terms that are changed by the shift at an electrode.

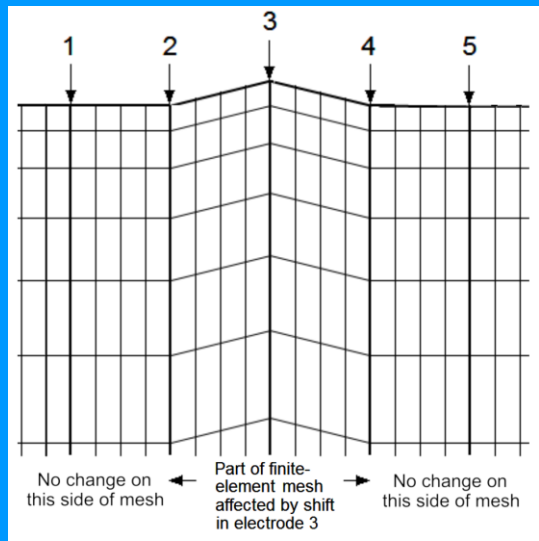

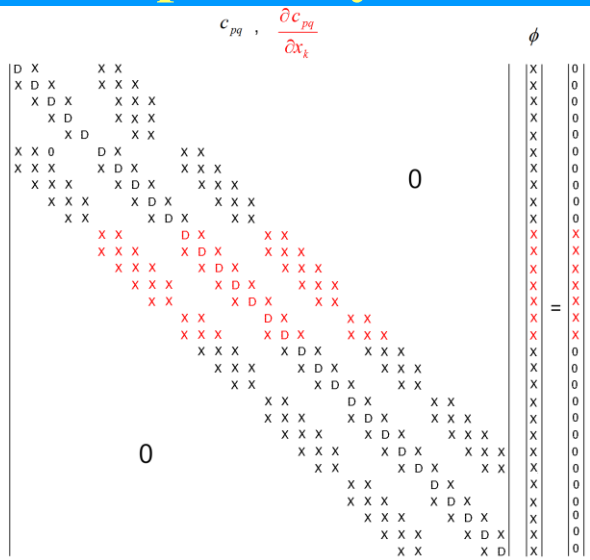

3-D mesh and spatial Jacobian matrix calculation

For 3-D problems, hexahedral finite elements are used. Each row in the C matrix has only 27 (or less) non-zero elements. A shift in an electrode position will only affect the mesh elements between it and 8 surrounding electrodes.

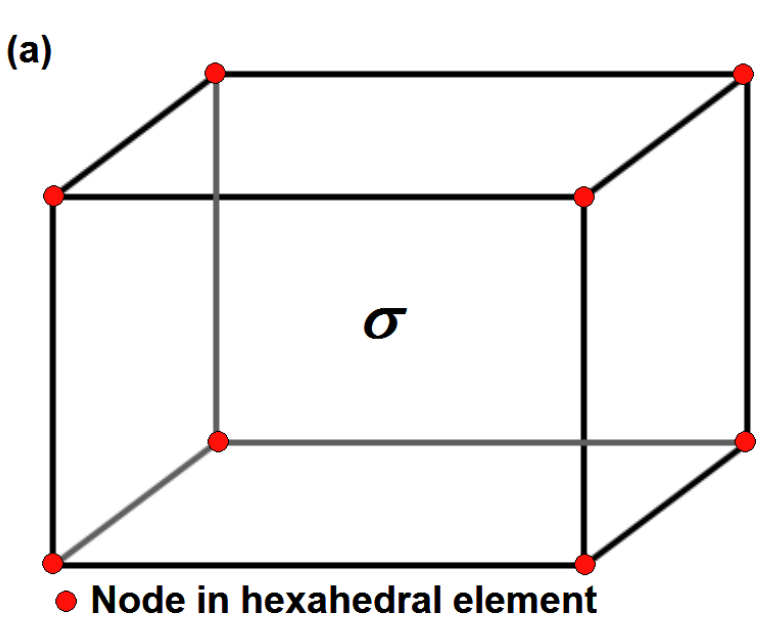

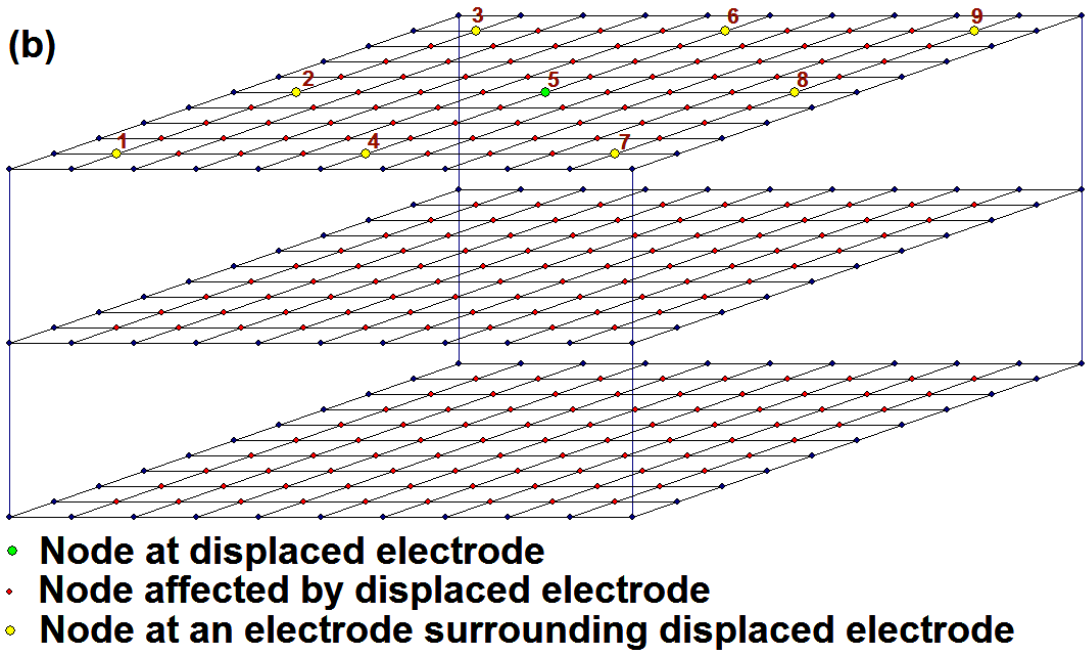

2-D model test and inversion with fixed electrodes

The model has a 500 Ω.m block and a deeper 20 Ω.m block in a 100 Ω.m medium. The perturbed model has 4 changes. One electrode (5m) is shifted horizontally, and another (17m) is shifted upwards. A 70 Ω.m prism is added, and 20 Ω.m prism is extended downwards. The data set consists of 415 dipole-dipole arrays. 1% voltage dependent random was added to the data.

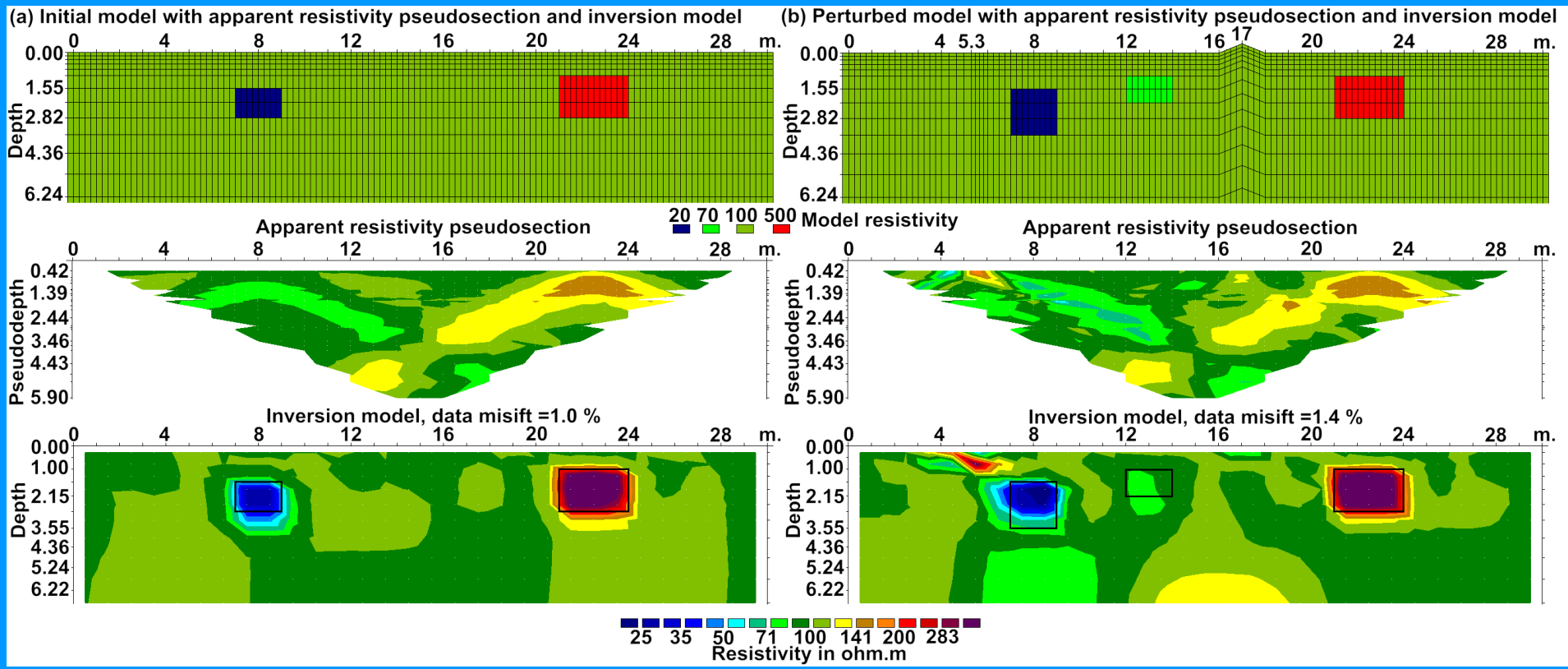

There is a good fit for initial model data set, but the perturbed data set model has large distortions near the 5m mark, and smaller distortions near the 17m mark.

Inversion model with variable electrodes

A homogenous half-space initial model is used. Tests were carried out using values of 1 to 100 for the relative spatial damping factors (α,β). The resistivity artifacts near the shifted electrodes were removed, but small values of α and β, there is a significant topographic distortion over the shallow high-resistivity block. It is reduced with higher damping factors, but with reduced accuracy in the electrode positions. The upwards shift at the 17m mark is reduced with increasing damping factors. Resistivity distortions start to appear for damping factors above 10.

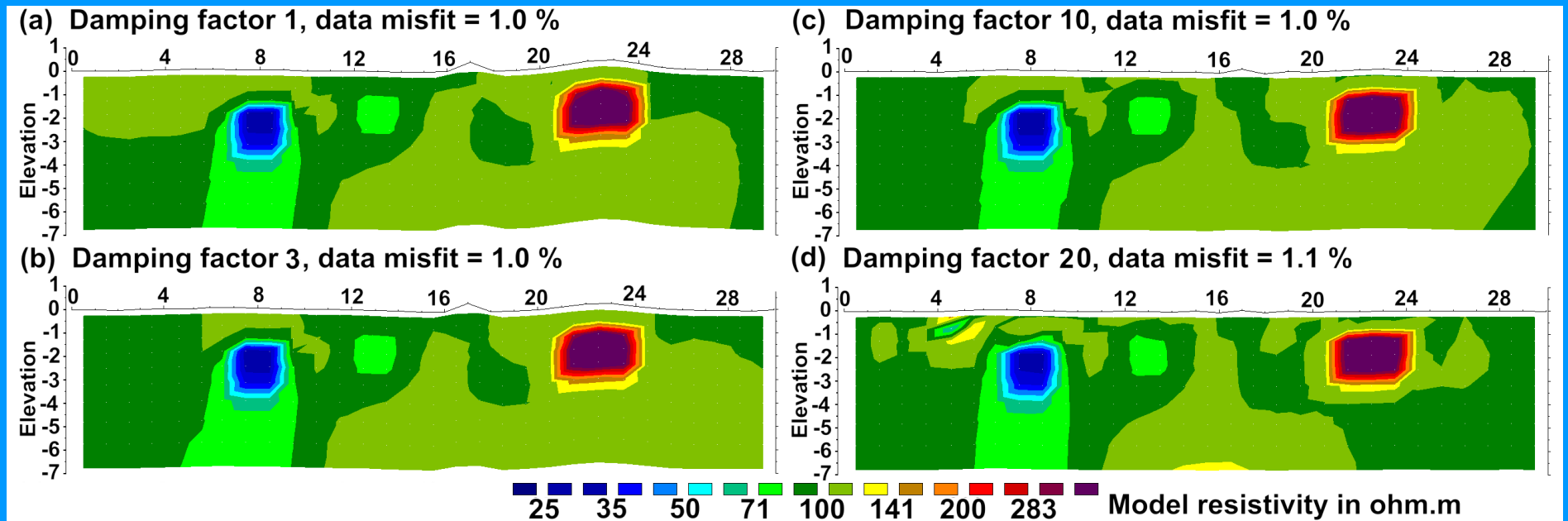

A closer look at the surface profile

The distortion in the surface profile over the high resistivity prism is clearly shown in the profile plot. The inversion algorithm is not able to fully distinguish between the anomalies due to effects of vertical shifts in the electrodes and a shallow subsurface resistivity structure. The distortion is reduced when the damping factor is increased. However, increasing the higher damping factor also decreases the elevation at the electrode at the 17 m mark compared to the true elevation (black line).

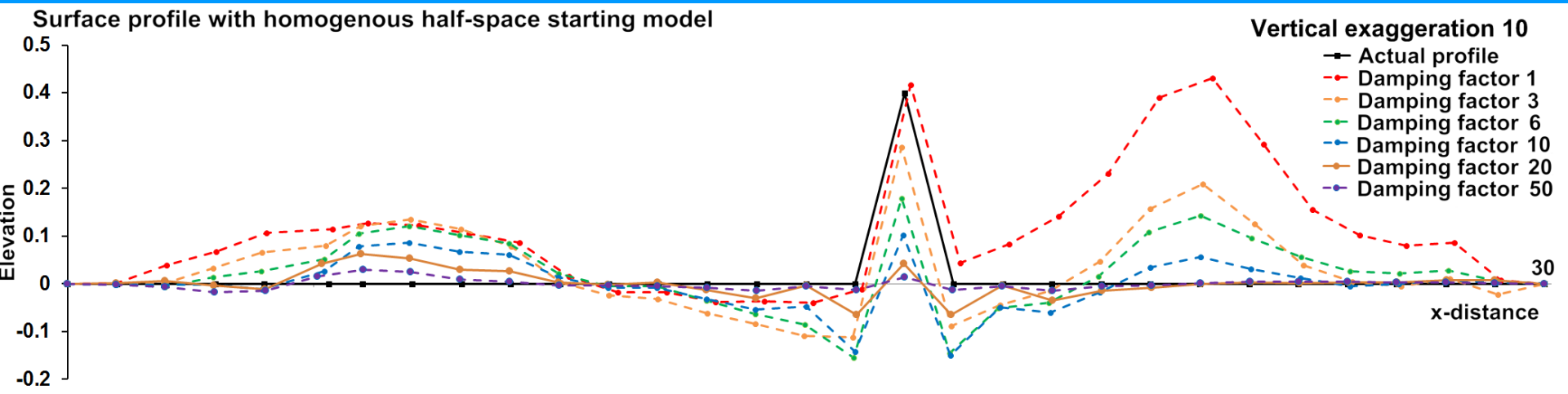

Method to reduce topographic distortions

Instead of using a homogenous half-space as the starting model, we use the model from the first time-lapse data set inversion with accurate electrode positions. The distortion over the high resistivity block is greatly reduced. Best damping factor value is between 1 to 6.

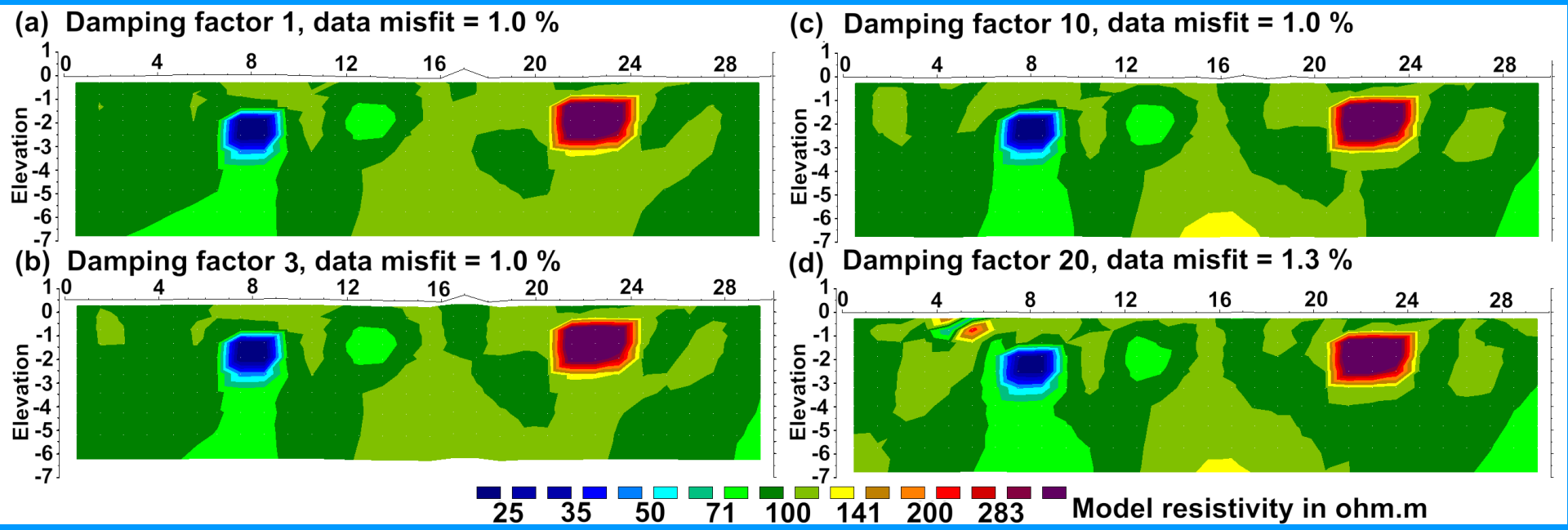

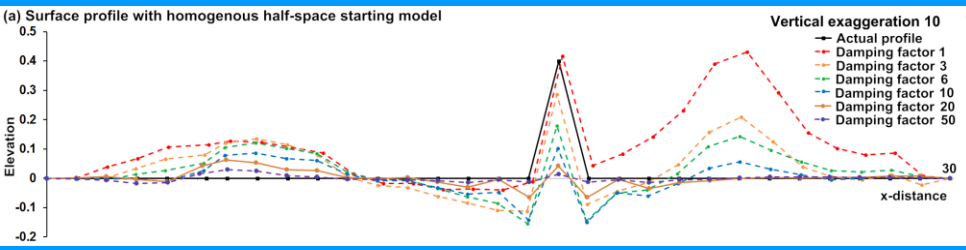

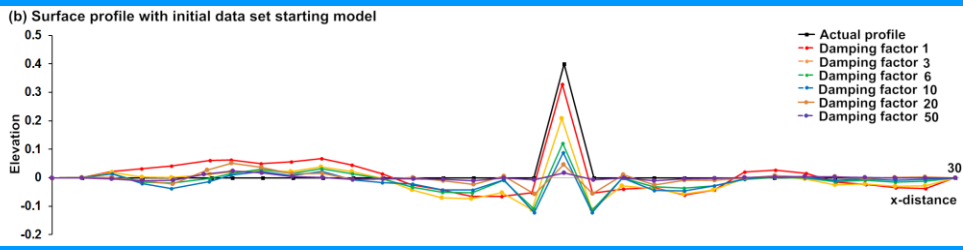

2-D and 3-D field data sets

The survey site is on Hollin Hill near Malton U.K. which has a mean slope of 14°. Slope failure occurs at a mudstone formation in the upper part of the slope. The electrodes were initially laid out along 5 lines each with 32 electrodes with an inline spacing of 4.75 m and 9.5 m between the lines. Measurements were made using the inline dipole-dipole and cross-line equatorial dipole-dipole arrays.

An automatic geophysical monitoring system that can make daily measurements since March 2008 was used. Direct measurements of the electrodes positions were made much less frequently. Failure of the slope was observed to occur occasionally.

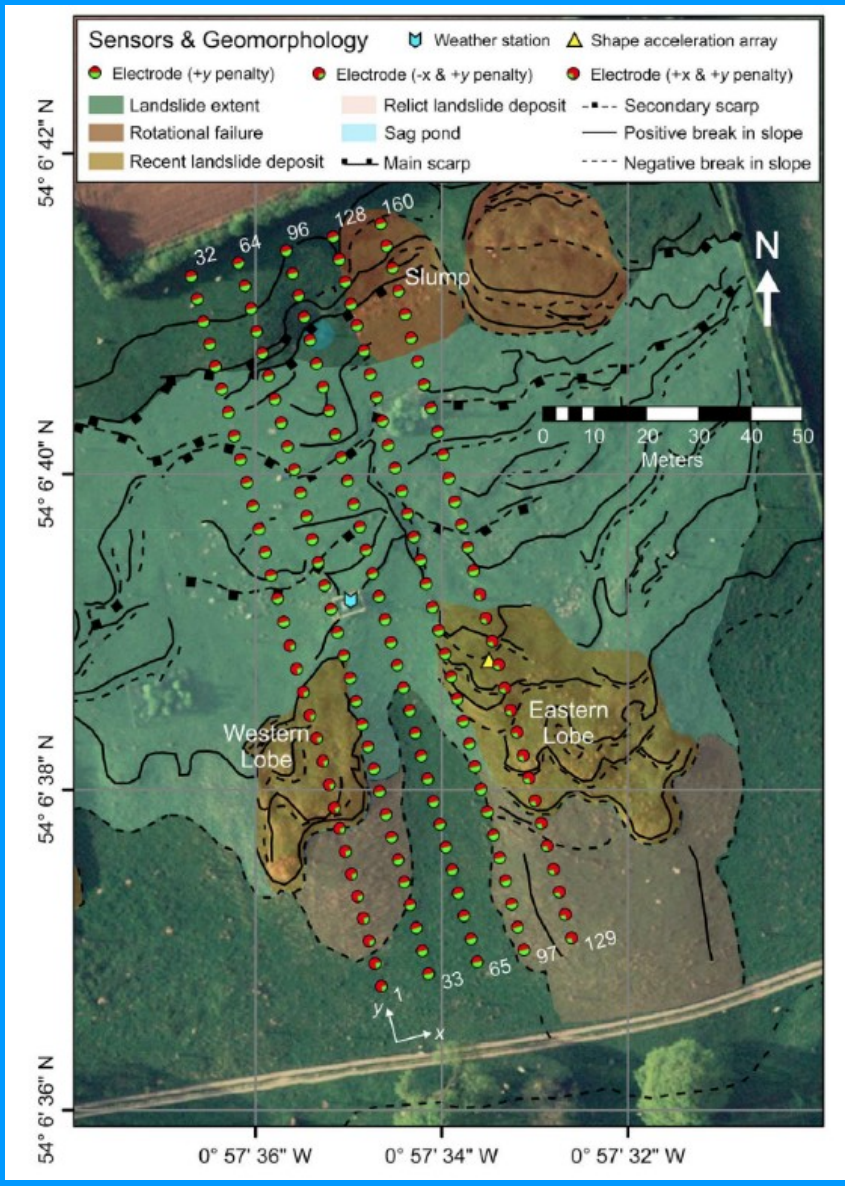

Hollin Hill : ground movement

A rectangular grid was originally laid out in March 2008. By Oct. 2010, some movement near electrode 9 had occured. Another survey from Feb. 2014 showed significant shifts at electrodes 157 to 160 (at the top of the slope) and 135 to 137, and slight movement near electrode 9.

The results from a 2-D survey along the western line is shown with the geology. The main formations are the Lias Group Redcar Mudstone Formation (RMF), Staithes Sandstone & Cleveland Ironstone Formation (SSF) and Whitby Mudstone Formation (WMF) which is the failing formation at the upper part of the slope.

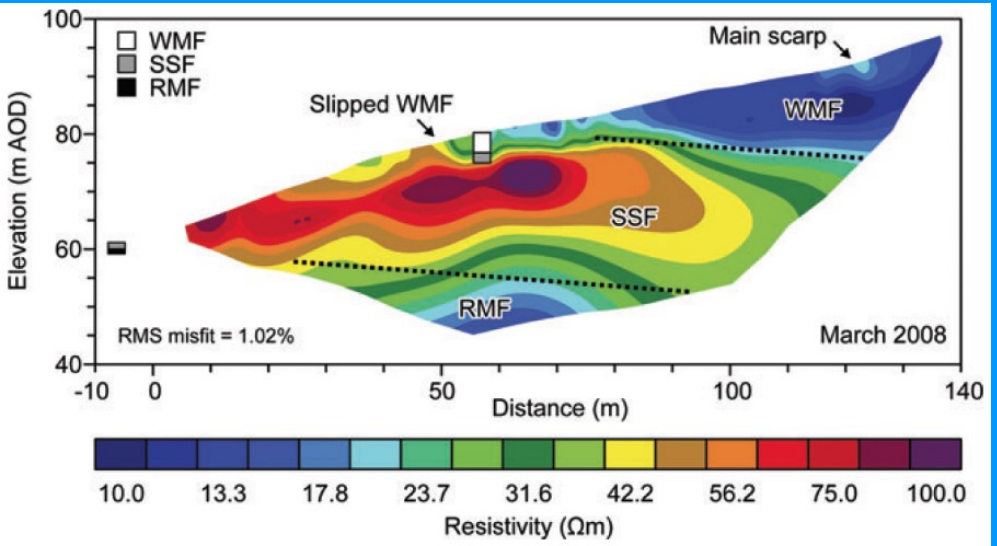

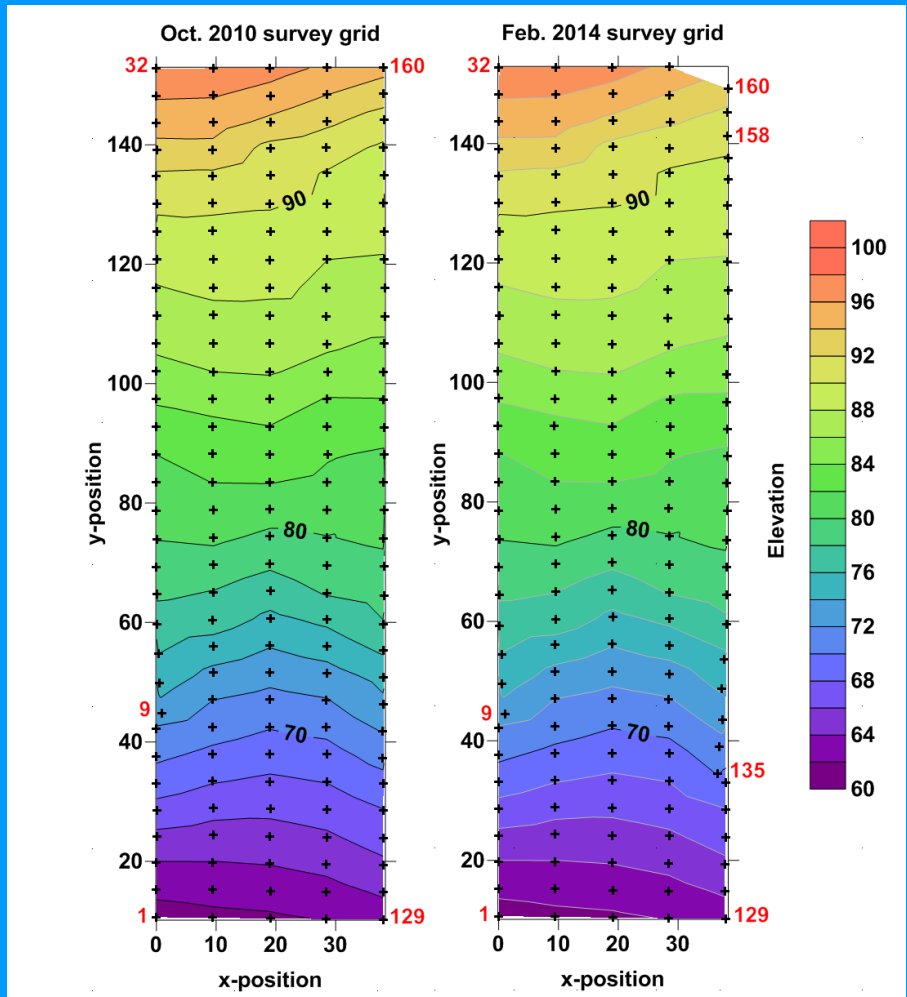

Hollin Hill : 2-D example

This example is from the western line of electrodes from surveys in March 2008 and March 2009. The inversion was carried out assuming fixed electrode positions from the March 2008 survey. There are significant near surface artifacts in the 2009 model due to movements near electrode 9.

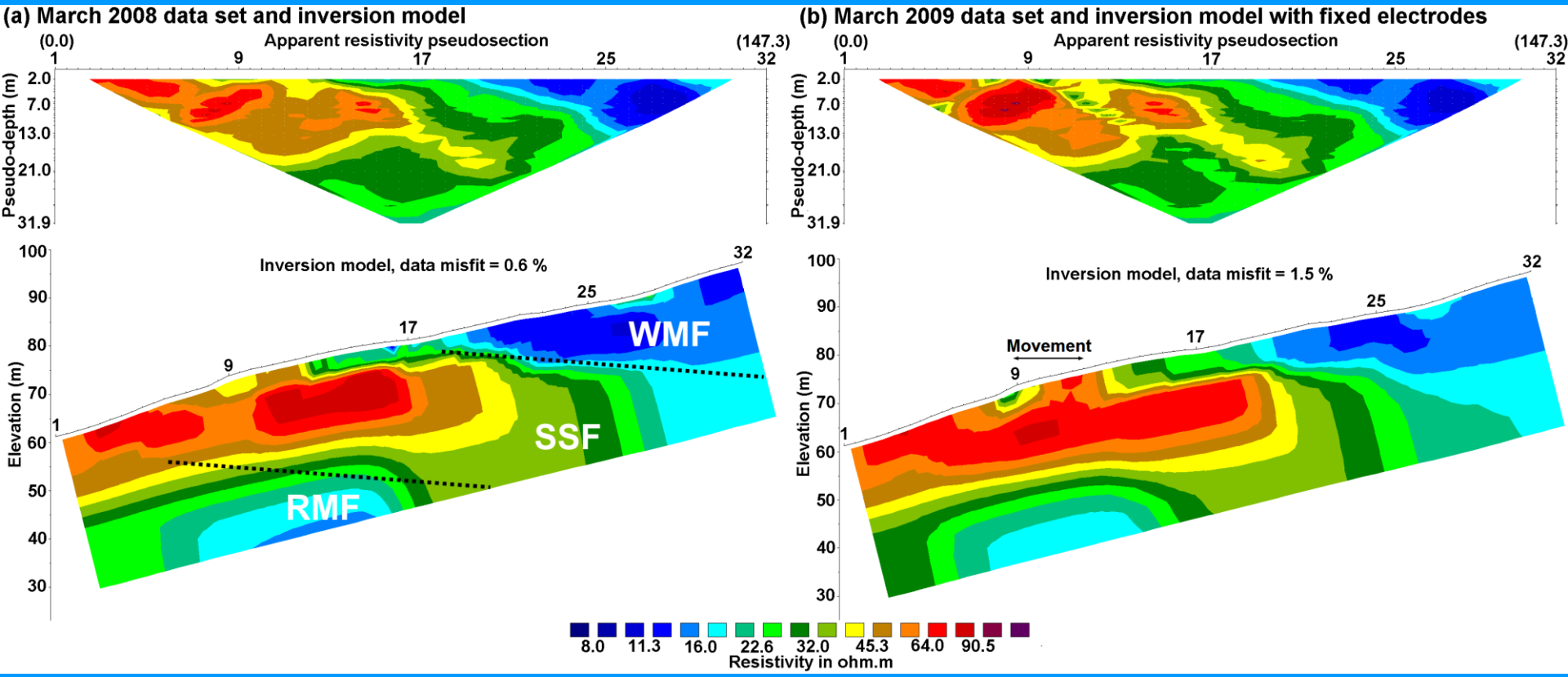

Hollin Hill – inversion with shifting electrodes

The inversion model for the 2009 data set where the electrodes are allowed to shift has removed the artefacts near electrode 9. The 2008 model was used as the starting model.

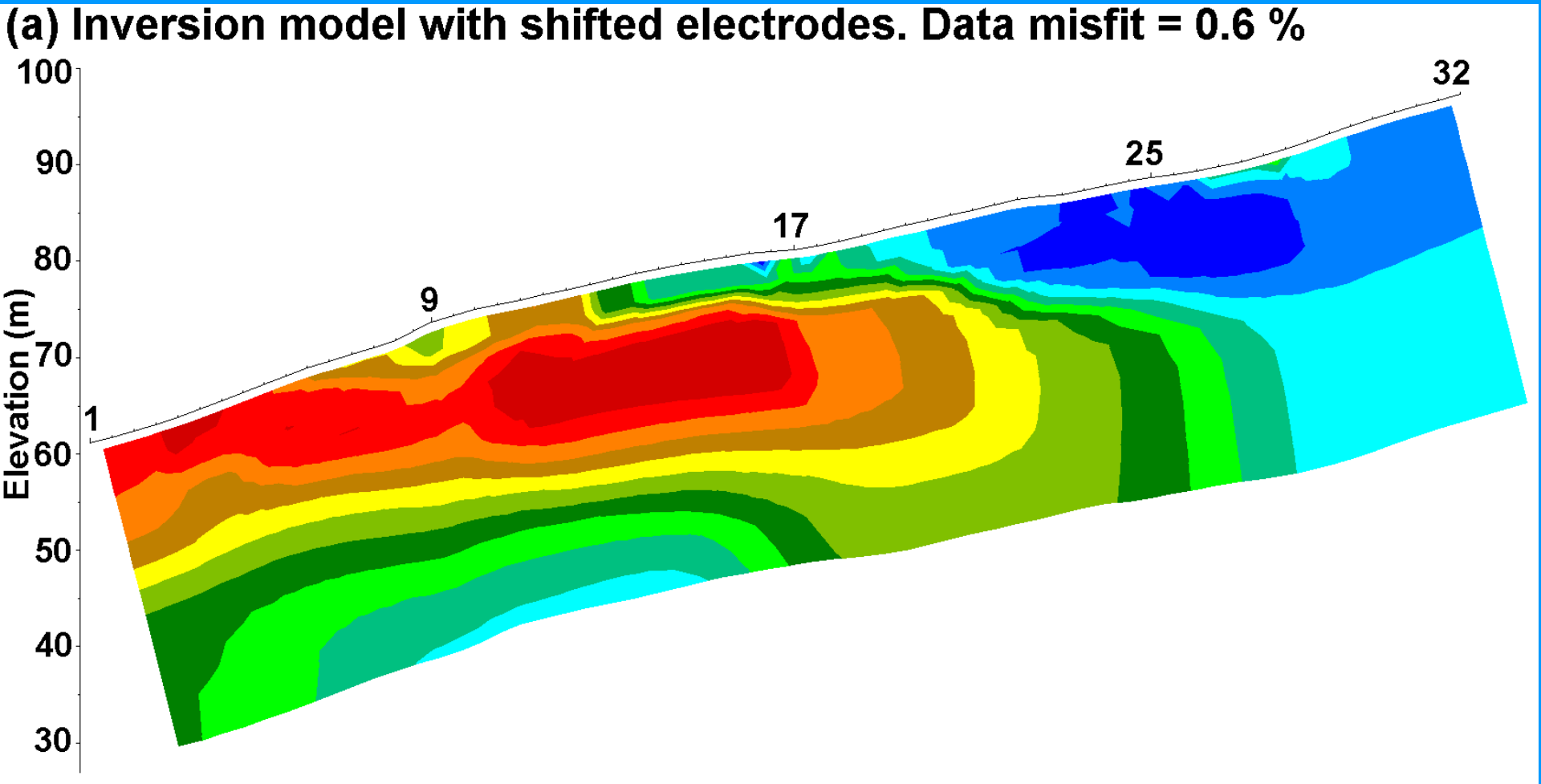

Hollin Hill – inversion with shifting electrodes

The 2009 inverse model electrodes profile (green rectangle) shows a slight shift upwards at positions 15 to 17 of up to 0.2 m. compared to the 2008 positions (blue circle), which is an artefact as they should only move downwards.

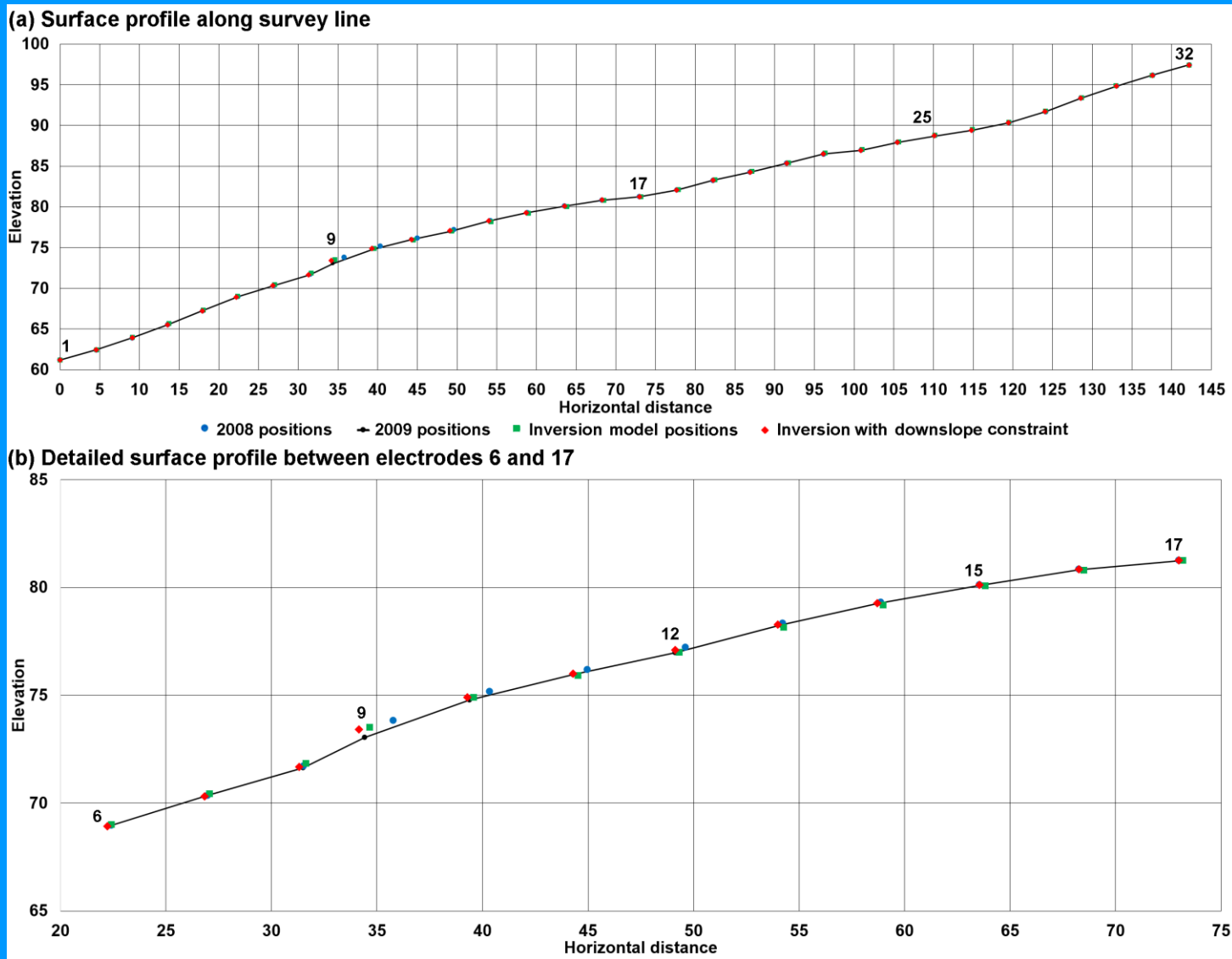

Constrained inversion for shifting electrodes

We can force the inversion to produce unidirectional shifts in the electrode positions by using the method of transformations. The variable for the horizontal position of an electrode, x_k, is replaced by a new variable, τ_k, as follows.

$$x_k = x_{ku} - \tau_k^2$$

x_{ku} is the upper limit for the kth electrode position. If this is set at the position of the electrode from the 2008 survey, it ensures that the new position of the electrode from the optimization routine will be less than the original position (i.e. downslope). This removes the small upslope shifts at electrodes 15 to 17 (b). The inverse model using the directly measured positions of the electrodes is also shown in (c). The differences between the models are not significant.

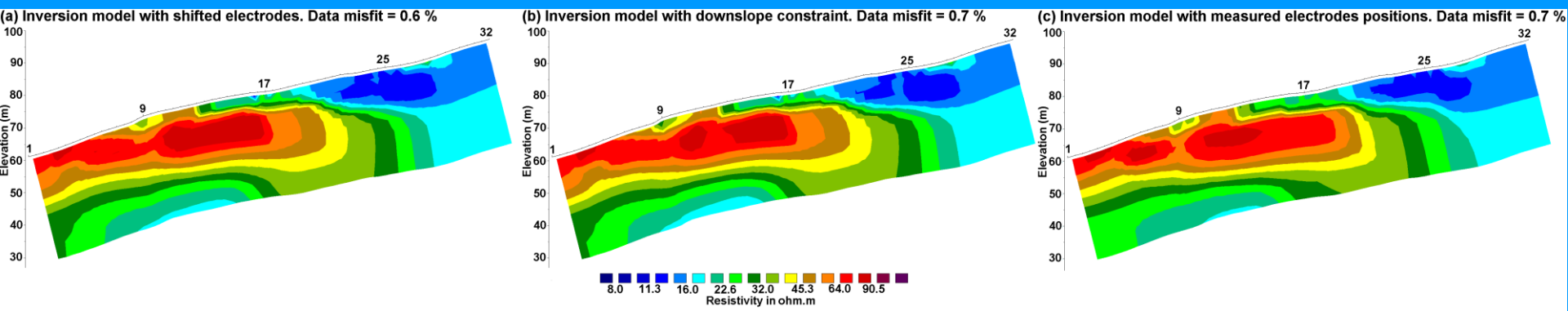

Constrained shifts inversion results

The RMS difference between the 2008 (blue) and 2009 (black) electrode positions is 0.37 m. The RMS difference in the estimated electrode positions (green) and the true 2009 positions is reduced from 0.19 m when the electrodes are allowed to shift. This is further reduced 0.12 m with the downslope constraint (red).

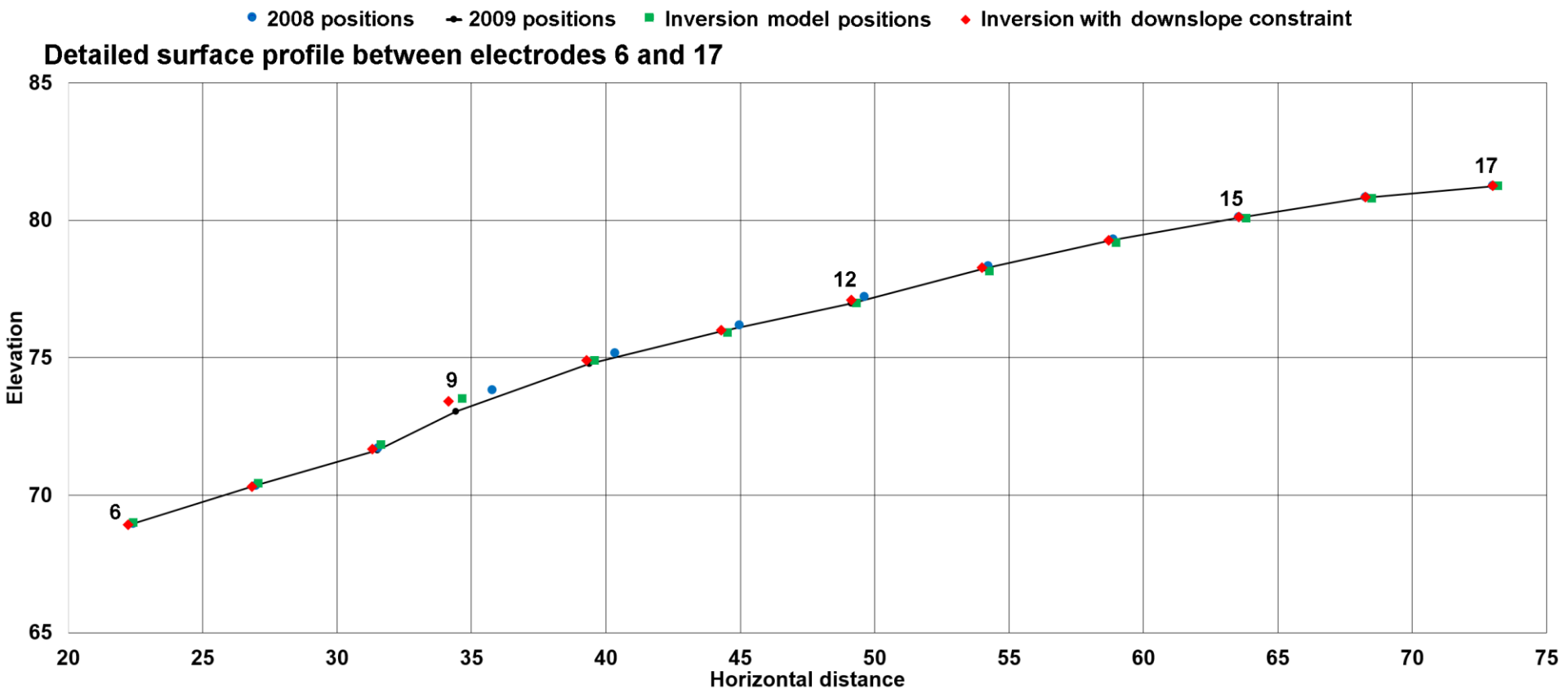

Hollin Hill : 3-D example

The data sets from surveys in 2010 and 2014 are used as examples. Measurements were made using the inline dipole-dipole (2262) and cross-line equatorial dipole-dipole (942) arrays. The inversion model from the survey carried out in Oct. 2010 is shown on the left in the form of layers starting from the top (a). The right side shows the model for the data from the Feb. 2014 survey using the electrode positions measured in 2010. Since this does not take into account movement of the electrodes during that period, there are significant false resistivity anomalies particularly at the lower right side of the top two layers in the 2014 model (b).

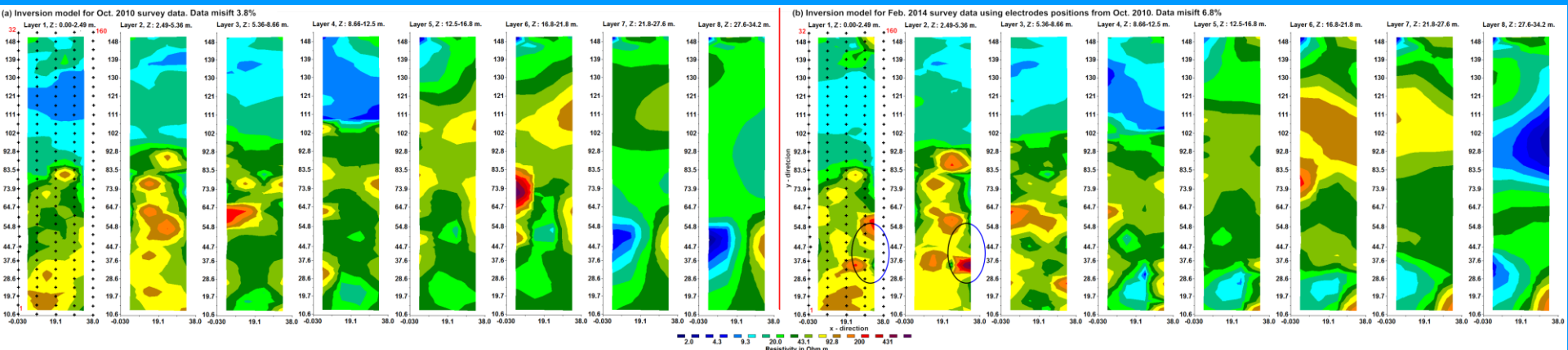

Hollin Hill : 3-D inversion with shifting electrodes

The inversion model where the electrodes are allowed to shift (b, right side) eliminates the resistivity artefacts between electrodes 136 to 138 compared to the model with fixed electrodes (a, left side). It also shows the downslope shift at electrodes 158 to 160. The amount of shifts in the model were 1.6, 1.8 and 1.1 m compared to the true values of 2.0, 3.2 and 3.8 m. The significantly smaller model shifts is probably because the electrodes are located near the top-right corner of the grid where there is less data. Furthermore it was found that the data from these electrodes was generally noisier than at other electrodes.

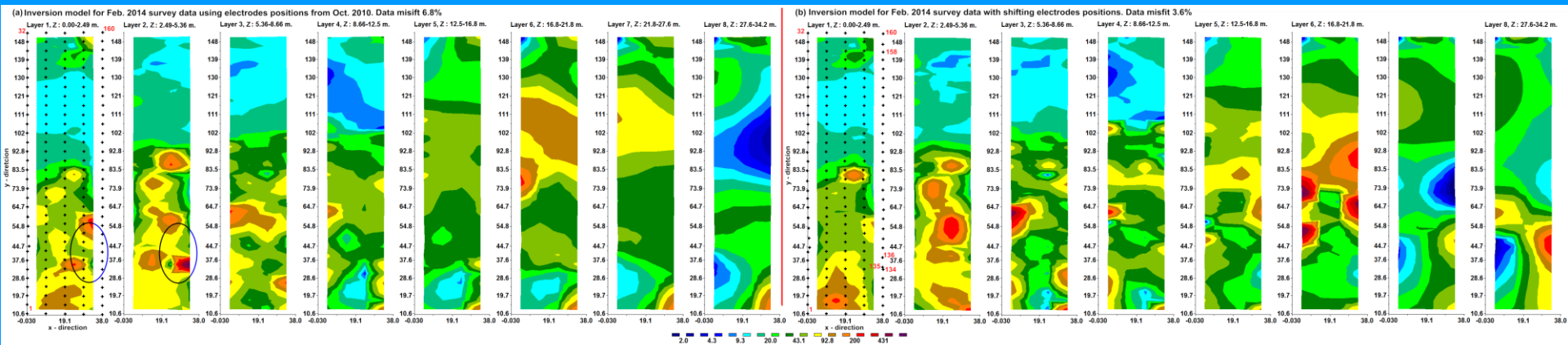

Hollin Hill : electrodes movement resolution plots

Model resolution plots are commonly used to estimate the reliability of the model resistivity values. The electrode positions resolution plots illustrate the degree to which we can estimate the movement of the electrodes in different directions from the data set. The values depend on the set of arrays used and the model resistivity. As the inline dipole-dipole arrays that constitute most of the data points are aligned in the y-direction, the y-resolution plot has the highest values. The z-resolution plot generally has the lowest values showing that vertical electrode shifts are poorly detected.

Surveys are usually designed to maximize the resolution of the subsurface resistivity. In landslide prone areas, they should also be designed to maximize resolution of the electrodes movements as well, if it is necessary to retrieve changes in the electrode positions from the apparent resistivity data.

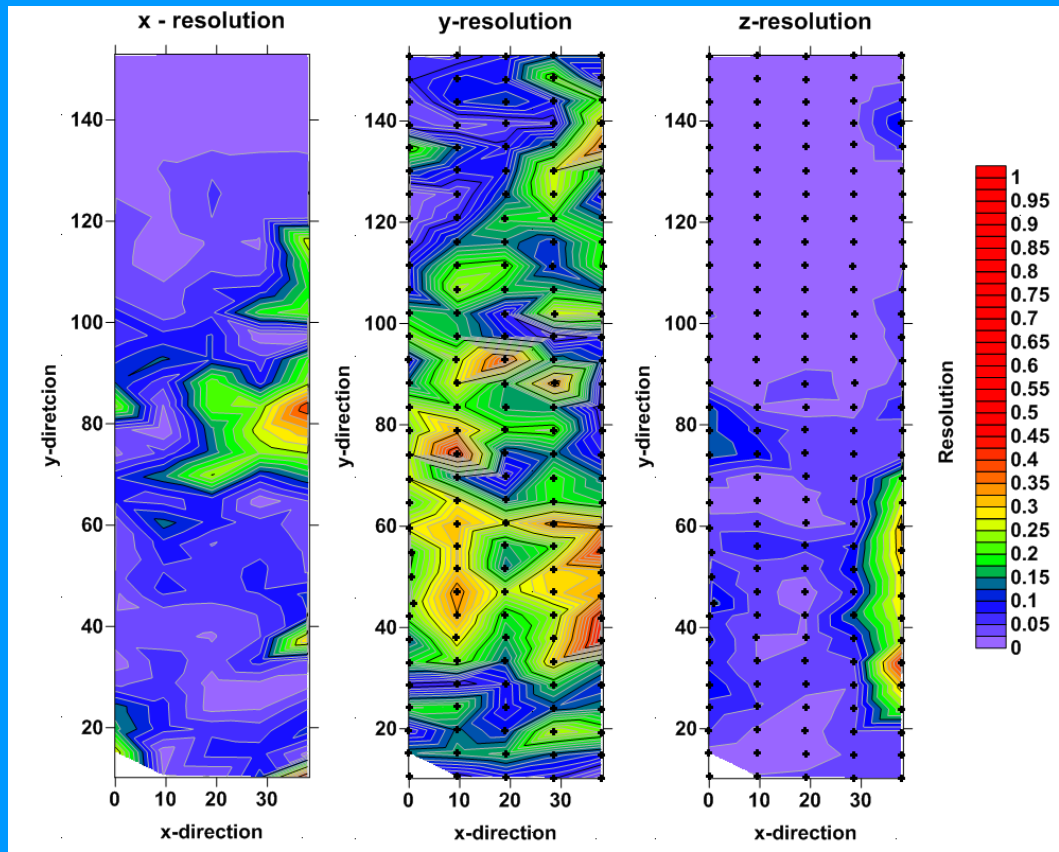

Conclusions

1. The least-squares inversion method can be modified to include the positions of the electrodes as model parameters. The direction of electrodes movement in the inverse model can by constrained by using the method of transformations.

2. The Jacobian matrix calculation time is greatly reduced by using the adjoint-equation method and taking into account the sparse nature of the finite-element capacitance matrix.

3. The accuracy of the recovered electrode positions can be greatly improved by using the inversion model from an initial data set (with known electrode positions) as the starting model for the inversion of a later time data set. This eliminates the effect of the common background resistivity variations.

4. Selection of arrays should also take into account their sensitivity to electrode movements so that they can be more accurately estimated from the apparent resistivity data.